Food & Function

PAPER

View Article Online
View Journal | View Issue

Cite this: *Food Funct.*, 2019, **10**, 3880

Red yeast rice ameliorates high-fat diet-induced atherosclerosis in *Apoe*$^{-/-}$ mice in association with improved inflammation and altered gut microbiota composition†

Yanhan Dong,‡[a] Huimin Cheng,‡[b] Ying Liu,[c] Meilan Xue [c] and Hui Liang *[b]

Received 19th March 2019,
Accepted 13th May 2019

DOI: 10.1039/c9fo00583h

rsc.li/food-function

Gut microbiota plays an important role in many metabolic diseases and has been linked to cardiovascular disease, including atherosclerosis. Clinical studies suggest that red yeast rice (RYR) has the potential to reduce blood lipid levels. However, the mechanisms under which RYR regulates atherosclerosis by affecting the composition of the gut microbiome have not been elucidated. In the current study, results showed that treatment with RYR significantly decreased the plaque formation and levels of cholesterol and low-density lipoprotein (LDL) compared with the atherosclerotic model group which were fed with a high-fat diet. In addition, the height of enteral villus in the red *Monascus* group was increased, indicating that RYR can improve the intestinal barrier function. Further analysis revealed that RYR might attenuate atherosclerosis through inhibiting hydroxy methylglutaryl-CoA reductase and the consequent inflammatory signaling pathways mediated by TLR2 and TLR4. Moreover, the RYR treatment led to significant structural changes on the intestinal microbiota of high-fat diet-fed mice and reduced the relative abundance of *Alistipes* and *Flavonifractor* that exhibited positive relationships with the plasma levels of cholesterol and LDL. Collectively, these findings illustrated that RYR could significantly protect against atherosclerosis, which was possibly associated with the alterations in the gut microbiota composition.

1. Introduction

Atherosclerosis is a major cause of cardiovascular mortality throughout the world, which is a chronic inflammatory disease accompanied by lipid disorders and plaque instability.[1] Atherosclerosis starts with lipid accumulation in the arteries and oxidation of low density lipoprotein (LDL) cholesterol that triggers the activation and participation of macrophages in the developing lesions.[2,3] It has been shown that the formation and rupture of atherosclerotic plaques are related to higher levels of gut microbiota-derived lipopolysaccharides (LPSs) and inflammatory cytokines in the circulation.[4,5]

In addition, Toll-like receptors (TLRs), which are a family of innate immune system receptors, have been identified as critical regulators in the development of atherosclerosis.[6] Stimulation of TLRs serves to initiate inflammatory signaling in response to pathogen-associated molecular patterns (PAMPs), which are highly conserved and present in bacteria, yeast, and viruses. For instance, TLR4 can recognize LPSs produced by gut microbiota and lead to rapid induction of inflammatory signaling cascades, including the interferon regulatory factor-3 (IRF-3)-dependent signaling pathway.[7] Recently, emerging evidence has highlighted that altered composition and function of gut microbiota is linked to obesity and cardiometabolic diseases.[8] Previous studies have revealed that a high-fat diet increases the levels of gut microbiota-derived trimethylamine-*N*-oxide (TMAO) into the circulation, and decreases the levels of short chain fatty acids (SCFAs) to abolish the effects of microbiota on host chromatin states, resulting in cardiovascular disease progression.[9,10] These findings suggest that high-fat diet-induced atherosclerosis could be reduced by targeting gut microbiota-induced chronic inflammation and intestinal barrier dysfunction.

Despite the widespread use of statin-based lipid-lowering therapies, the global burden of this disease remains high.[11] Therefore, more attention is paid to investigate novel therapeutic strategies. Red yeast rice (RYR), which is produced by cultivating the yeast species *Monascus purpureus* on rice, has

[a]*Institute for Translational Medicine, Qingdao University, Deng Zhou Road 38, Qingdao 266021, China*
[b]*Department of Human Nutrition, College of Public Health, Qingdao University, Deng Zhou Road 38, Qingdao 266021, China. E-mail: qdlianghui@126.com; Tel: +86-532-83812357*
[c]*Basic Medical College, Qingdao University, Deng Zhou Road 38, Qingdao 266021, China*

†Electronic supplementary information (ESI) available. See DOI: 10.1039/c9fo00583h

‡The authors contributed equally to this work.

been used as a food supplement or herbal medicine in Eastern Asia for several centuries. It contains a variety of functional secondary metabolites, such as sterols, isoflavones, pigments, monacolin K, and yeast polyketides.[12] Clinical studies have found that red yeast rice has potential to reduce serum levels of LDL and cholesterol (CHOL).[13,14] However, the underlying mechanisms by which RYR inhibits atherosclerosis and the association with the modulation of gut microbiota remain poorly understood.

Here, this study aimed to evaluate the effects of RYR supplementation in a high-fat diet in terms of several atherosclerosis parameters and the contribution of intestinal gut microbiota in *Apoe*$^{-/-}$ mice. Our results indicate that RYR might reduce the development of atherosclerosis by manipulating the gut microbiota composition.

2. Methods

2.1 Animals

In this study, all procedures involving animals were reviewed and approved by the Institutional Animal Care and Use Committee of Qingdao University Medical College. All animal procedures were performed in accordance with the Guidelines for Care and Use of Laboratory Animals of Qingdao University and approved by the Animal Ethics Committee of Qingdao University. Seven-week-old male *Apoe*$^{-/-}$ mice on a C57BL/6J background (B6.129P2-*Apoe*^{tm1Unc}/J) were purchased from Beijing Vital River Laboratory Animal Technology Co., Ltd [Beijing, China, certificate No. SCXK (Jing) 2016-0011]. After a one-week acclimatization period, mice were divided into three groups: normal diet without RYR treatment, high-fat diet (containing 15% fat and 0.25% cholesterol) with saline, and high-fat diet with RYR (0.34 g kg^{-1} day^{-1}, Hangzhou Hetian Biotechnology Co., Ltd, China) treatments. The RYR was dissolved in distilled water and administered once daily by oral gavage. All animals were provided *ad libitum* access to food and water and housed under the conventional 12 h:12 h light/dark cycle for 12 weeks. The time-series data of the body weight are given in Table S1.† The plasma total cholesterol, triglyceride (TG), and LDL levels were measured at 0, 4, 8, and 12 weeks from the beginning of the experiment. At the end of the experiment, all mice were sacrificed by a sodium pentobarbital overdose. The hearts, artery tissues, livers, and intestinal contents were collected for further processing.

2.2 Analysis of atherosclerotic lesions

After collection of blood samples, the circulatory system was rinsed with phosphate-buffered saline (PBS) and then fixed with PBS containing 4% paraformaldehyde. To evaluate atherosclerotic lesion areas, the aorta was cut longitudinally to expose the intimal surface, and the plaque-containing area was stained with Oil Red O. Lesions in the aortic area were quantified from the aortic arch to the iliac bifurcation. The ascending aorta was sectioned (8 μm) serially and then stained with Oil Red O. Lesion images were captured with a microscope (Olympus, Tokyo, Japan). The lesion area and size were quantified using Image J software by a blinded observer.

2.3 Aorta and colon examination by transmission electron microscopy

Aortic roots and intestinal tissues were immediately fixed after sacrifice by immersing them in 2.5% glutaraldehyde in 0.1 mol L^{-1} PBS for 4 h. The samples were then washed three times and post-fixed in 2% osmium tetroxide, dehydrated using a standard series of ethanol and propylene oxide concentrations, and then embedded in epoxy resin. One-micrometer sections were stained with methylene blue, and MG tissues were then sectioned on an ultratome (LKB; Gaithersburg, MD, USA) with a diamond knife. Sections were collected on 150-mesh grids, stained with uranyl acetate and lead citrate, examined and photographed using a transmission electron microscope (JEM-1200 EX; JEOL, Tokyo, Japan). The lengths of enteral microvilli were measured from at least three separate transmission electron microscope images using Image J software.

2.4 Immunoblot

Immunoblot was performed as described.[15] In brief, the tissues were lysed for 1 h at 4 °C in a lysis buffer (20 mM Tris [pH 7.5], 2 mM EDTA, 3 mM EGTA, 2 mM DTT, 250 mM sucrose, 0.1 mM PMSF, 1% Triton X-100 and a protease inhibitor cocktail). The samples were subjected to 12% SDS-PAGE and transferred to nitrocellulose membranes. Equal-protein loading was controlled by Ponceau red staining of the membranes. Blots were probed using antibodies. The anti-NF-κB antibody (Abcam, ab32536, 1 : 1000), anti-TNF-α antibody (ABclonal, A11534, 1 : 1000), anti-IL-1β antibody (Bioss, bs0812R, 1 : 1000), anti-HMG-CoA reductase antibody (ABclonal, A16875, 1 : 1000), anti-occludin antibody (Proteintech, 27260-1-AP, 1 : 300), anti-JAM-1 antibody (ABclonal, A1241, 1 : 1000), anti-TLR2 antibody (ABclonal, A11225, 1 : 500), anti-TLR4 antibody (Boster, BA1717, 1 : 200), and anti-MAP-kinase antibody (Proteintech, 14064-1-AP, 1 : 1000) were used in this study. After incubation with the primary antibody, the secondary antibodies were added. The horseradish peroxidase-conjugated goat anti-rabbit or goat anti-mouse IgG was purchased from Santa Cruz Biotechnology. Western blot bands were quantified using the ImageJ software. Three samples per group were selected to perform three independent experiments.

2.5 Gut bacterial DNA extraction and high throughput sequencing

Caecal contents were used for DNA extraction with a QIAamp Fast DNA Stool Mini Kit (Qiagen) according to the manufacturer's protocols, as described.[16] The extracted DNA was amplified with primers targeting the V3–V4 region of bacterial 16S rRNA genes (forward: 5-CCT ACG GRR BGC ASC AGK VRV GAA T-3; reverse: 5-GGA CTA CNV GGG TWT CTA ATC C-3). Sequencing was performed on the platform of Illumina HiSeq

2000, and the analysis was carried out by Ruiyi Biotechnologies Inc. (Shanghai, China).

2.6 Bioinformatic analysis

The raw reads were quality filtered and merged using Pandaseq.[17] Then, based on Ribosomal Database Project (RDP), the sequence reads were classified into operational taxonomic units (OTUs) using Usearch with a 97% similarity cutoff.[18] The taxonomy analysis was performed on Illumina's BaseSpace cloud computing platform. Two-dimensional principal component analysis (PCA) plots were drawn using the SIMCA-14.1 software (UMETRICS, Sweden) based on the relative abundance of gut microbiota at an OUT level. Taxonomic changes that differed significantly between the different groups were analyzed by the linear discriminant analysis (LDA) effect size (LEfSe) algorithm through the LEfSe Tools.[19] The correlation network between lipid metabolic disorders-related indexes and the intestinal microbiota was visualized by an open source software platform (http://www.cytoscape.org/).

2.7 Statistical analysis

Statistical analyses were performed with Statistical Package for Social Sciences (SPSS). All data are expressed as the means ± standard deviation (SD). The Kruskal–Wallis test with Bonferroni *post hoc* tests was used to analyze nonparametric data; one way ANOVA with *LSD-t* tests were used to analyze parametric data. Statistical tests were done using GraphPad Prism 5. Value of $p < 0.05$ indicated statistical significance.

3. Results

3.1 Red yeast rice significantly reduced high-fat diet-induced atherosclerotic lesion formation in *Apoe*$^{-/-}$ mice

To explore the possible role of red yeast rice in atherosclerosis, *Apoe*$^{-/-}$ mice fed with the high-fat diet were treated with saline or RYR by oral gavage daily for a period of 12 weeks. The high-fat diet group induced the formation of atherosclerotic plaques compared with the control group, while treatment with RYR substantially reduced the plaque area by approximately 15% in *Apoe*$^{-/-}$ mice fed with the high-fat diet (Fig. 1A and B). Moreover, the lesion area at the ascending aorta was significantly decreased in the RYR-treated group than in the high-fat group (Fig. 1C and D).

3.2 Treatment with RYR improved lipid metabolism and prevented the high-fat diet-induced effects on structure of enteral tissue

Compared with the control group, the plasma levels of total CHOL and LDL were significantly increased in the high-fat diet group (Fig. 1E), whereas the daily oral gavage with RYR had significantly reduced the levels of plasma CHOL and LDL as compared to the control group and the high-fat diet group. However, there were no obvious changes in the plasma level of TG between the three groups.

We also observed the ultrastructure of the arterial tissues and small intestine by transmission electron microscopy. In the model group, there was intima thickening accompanied by a slight loss of endothelial cells, autophagosomes, atherosclerotic plaque formation, atrophy of the media, and a completely elastic membrane in contrast with the control group. However, RYR treatment significantly reduced the harmful effect with intact endothelial cells, and the medial membrane was not pathologically altered (Fig. 1F). The results of Fig. 1G showed that the enteral microvilli were abundant and arranged neatly in the control group. The columnar epithelial cells were structurally intact and the intercellular junction structure was basically normal. Compared with the control group, the junction of the high-fat diet group was relaxed, and the desmosome connection was unclear. In addition, the length of the microvilli was significantly shortened by 53.52% compared with the control group. In the RYR group, the intercellular junction structure was basically normal, and the microvilli length dramatically increased by 47.62% compared with the model group.

3.3 RYR ameliorated the inflammation in high-fat diet-fed *Apoe*$^{-/-}$ mice

Considering that the red yeast rice constituent monacolin K is an inhibitor of hydroxy methylglutaryl-CoA (HMG-CoA) reductase, it directly targets low-density lipoproteins to tackle the atherosclerotic plaque formation.[20] Thus, we examined the expression of HMG-CoA reductase in the liver. Treatment with RYR resulted in a significant decrease in protein levels of HMG-CoA reductase (Fig. 2A).

Tight junctions between adjacent endothelial cells can modulate vascular homeostasis.[21] In addition, there is an intestinal permeable barrier achieved by intercellular tight junction structures, which limits the permeation of noxious molecules into blood circulation to trigger inflammation.[22] The permeability of endothelial junctions is maintained by junction proteins, including JAM-1 and occludin. In the current study, the expression levels of JAM-1 and occludin proteins in the intestinal tissue of the *Monascus* group were significantly increased compared with the high-fat diet group (Fig. 2B), indicating that red yeast rice can improve enteral functions in *Apoe*$^{-/-}$ mice.

Compared with the control group, the protein levels of TNF-α and IL-1β were significantly increased in the model group, whereas treatment with RYR decreased the levels of TNF-α and IL-1β (Fig. 2C). The results suggested that red yeast rice could reduce the levels of inflammatory factors.

As we know, TLRs serve to initiate inflammatory signaling in response to detection of microbial PAMPs, which play a critical role in the development of atherosclerosis.[6] TLRs lead to rapid induction of inflammatory signaling cascades, including MAP-kinase and NF-κB activation, and thereby expression of inflammatory and atherogenic genes.[6] We analyzed the expressions of TLR2, TLR4, NF-κB, and MAPK in the aorta and found that the protein levels of TLR2, TLR4, and MAPK were

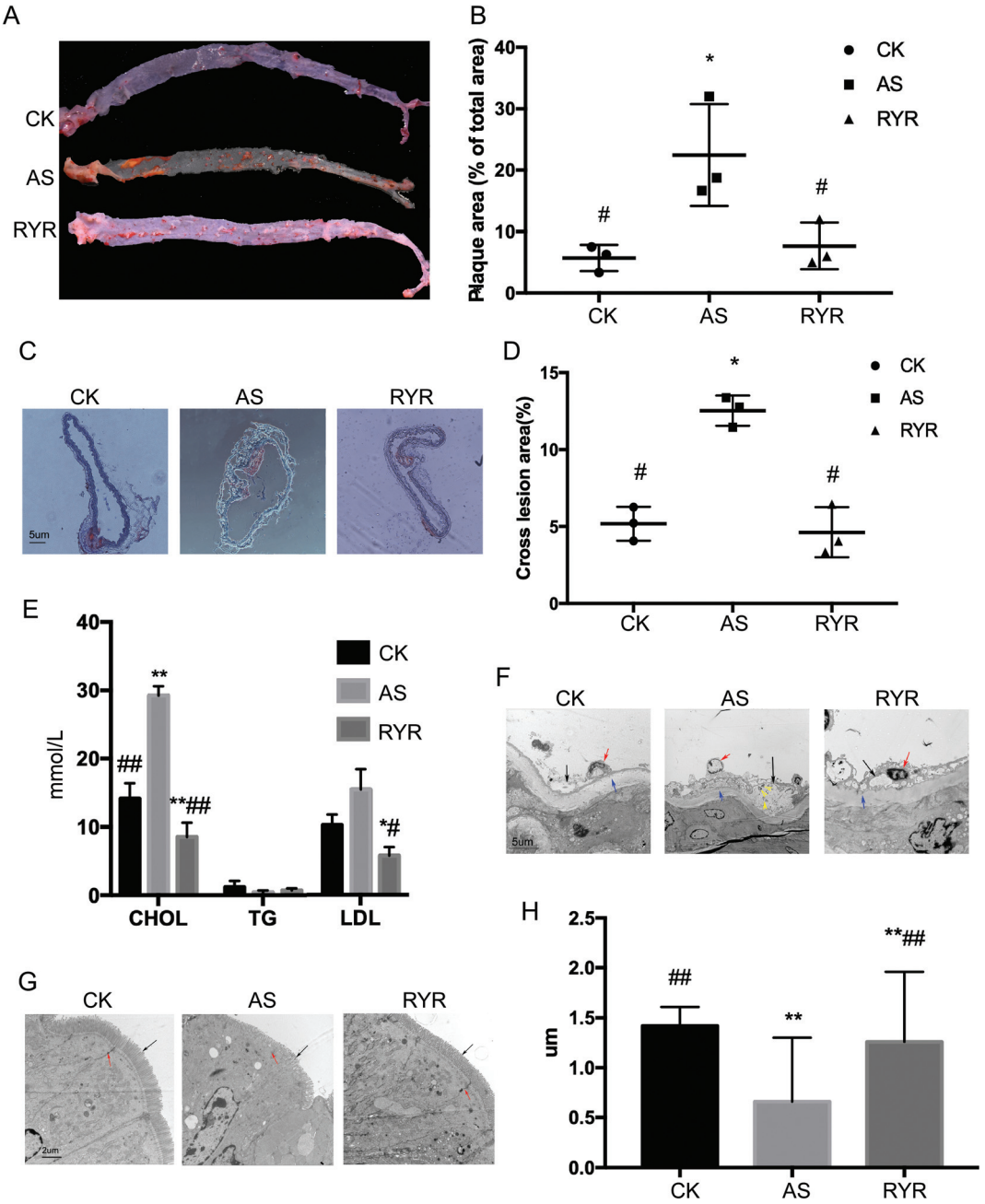

Fig. 1 High-fat diet-fed *Apoe*$^{-/-}$ mice treated with red yeast rice exhibited reduced atherosclerosis. Eight-week-old *Apoe*$^{-/-}$ mice were fed either a normal diet (CK, control group) or a high-fat diet (AS, atherosclerotic model group) for 12 weeks. The high-fat diet-fed mice were further separated into 2 groups: a group receiving daily oral gavage with RYR (RYR) and a group receiving daily oral gavage with saline as vehicle control. A, Representation of en face Oil Red O staining of aortic specimens. B, Quantitative analysis of plaque area in aorta (n = 6). C, Assessment of aortic atherosclerotic lesions through Oil Red O staining, and the quantitative analysis of the lesion area are shown in D (n = 6). Bar = 5 μm. E, Effects of RYR administration on the plasma CHOL, TG, and LDL levels in *Apoe*$^{-/-}$ mice fed with the high-fat diet for 12 weeks. F, Observation of the ultrastructure of arterial tissues by transmission electron microscopy. The black arrows indicate the atherosclerotic plaques; the red arrows indicate endothelial cells; the yellow arrows indicate autophagosomes; and the blue arrows indicate the medial membrane. Bar = 5 μm. G, Observation of the enteral microvilli by transmission electron microscopy. The black arrows indicate the enteral microvilli, and the red arrows indicate he intercellular junction structure. Bar = 2 μm. H, Quantitative analysis of the length of microvilli using Image J. Significant difference of AS from the CK group is denoted by *p < 0.05, **p < 0.01; significant difference of the RYR and CK groups from the AS group is denoted by #p < 0.05, ##p < 0.01.

significantly increased in the model group, whereas treatment with RYR decreased the levels of the three proteins (Fig. 2D). However, treatment with RYR had no obvious effect on the expression of NF-κB, indicating that RYR might prevent atherosclerosis through modulating TLR initiated MAPK signaling cascades.

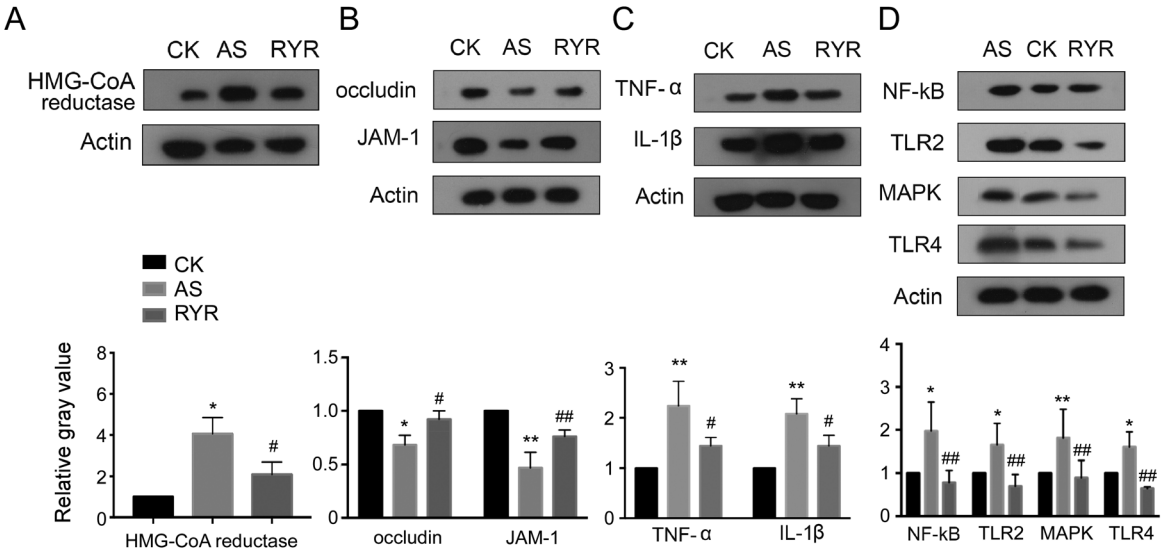

Fig. 2 RYR inhibited the inflammation in high-fat diet-fed *Apoe*$^{-/-}$ mice. Expression of HMG-CoA reductase in the liver (A), JAM-1 and occludin in the intestinal tissue (B), TNF-α and IL-1β in the intestinal tract (C), and the TLRs-initiated inflammatory signal pathway in the aorta (D) were detected by western blot, respectively. The respective quantitative results are also shown, which were calculated in three independent experiments. Significant difference of the AS group from the CK group is denoted by *$p < 0.05$, **$p < 0.01$; significant difference of the RYR group from the AS group is denoted by #$p < 0.05$, ##$p < 0.01$.

3.4 The effect of RYR treatment on gut microbiota

To investigate the effect of RYR treatment on the gut microbiota composition, we conducted Illumina HiSeq 16S rRNA gene sequencing, which produced 205 252 855 clean reads from 14 samples. As mentioned in previous studies,[5,23] the phylum-level composition was dominated by three phyla (*Bacteroidetes*, *Firmicutes*, and *Proteobacteria*), accounting for approximately 93% of the gut bacterial community. The degrees of OTUs (operational taxonomic units) shared between the three groups are summarized in the Venn diagram (Fig. 3A), which shows that 300 OTUs were common to three groups while some OTUs were still unique to each group (30 for the control group, 24 for the model group, and 54 for the RYR group, respectively), revealing a more OTU diversity in the RYR group. The Shannon index suggested that the gut microbiota diversity was markedly reduced by RYR treatment under the high-fat diet (Fig. 3B). In addition, the alpha diversity of the RYR group is relatively consistent with the control group. Principal coordinate analysis based (PCoA) on weighted-UniFrac distance demonstrated a clear variation in the microbiota composition of the high-fat diet group compared to the control and RYR groups, which account for 72.35% of the gut microbiota profile (Fig. 3C). Furthermore, the weighted-UniFrac NMDS (nonmetric multidimensional scaling) analysis revealed that the gut microbiota communities of the RYR group aggregated more closely to that of the control group compared to the high-fat diet group (Fig. 3D).

At the phylum level, there were no significant changes in the abundance of *Bacteroidetes* among the three groups. The abundance of *Firmicutes*, which often increases during obese states,[23,24] was markedly decreased by supplementing RYR compared to the high-fat diet group (Fig. 4A and B). At the family level, the abundance of *Rikenellaceae* was markedly decreased by supplementing RYR compared to the high-fat diet group, whereas the abundance of *Bacteroidaceae* was markedly increased by supplementing RYR compared to the control group (Fig. 4C and D).

To shed light on the bacterial phenotypes that contributed to the differences in gut microbiota communities, we employed the LEfSe analysis and demonstrated 17 gut bacterial clades with significant differences (Fig. 5A). The phylum of *Tenericutes* and *Anaeroplasmataceae* (from class to family) was found to be enriched in the RYR group. In addition, the abundance of the genus *Bacteroides* was also significantly increased by RYR, while the *Alistipes* abundance was markedly increased in the high-fat diet group (Fig. 5B). Furthermore, we investigated 14 genera which were considered as key genera responsible for the significant difference among the three groups (Fig. 5C). Compared with the high-fat diet group, the feature of the RYR group was characterized by a lower abundance of *Alistipes*, *Barnesiella*, and *Flavonifractor*, as well as a higher abundance of *Bacteroides* and *Anaeroplasma* (Fig. 5C).

In order to explore the correlations between the atherosclerotic parameters and the gut microbiota, we employed the Spearman's correlation analysis (Fig. 5D). The high-fat diet group that was enriched in *Alistipes*, *Clostridium IV*, *Eisenbergiella*, and *Flavonifractor* exhibited positive relationships with the plasma levels of CHOL and LDL. The relative abundance of *Erysipelotrichaceae* was found to be positively correlated with the plasma CHOL and LDL levels, the atherosclerosis lesion area, the liver HMG-CoA reductase level, and

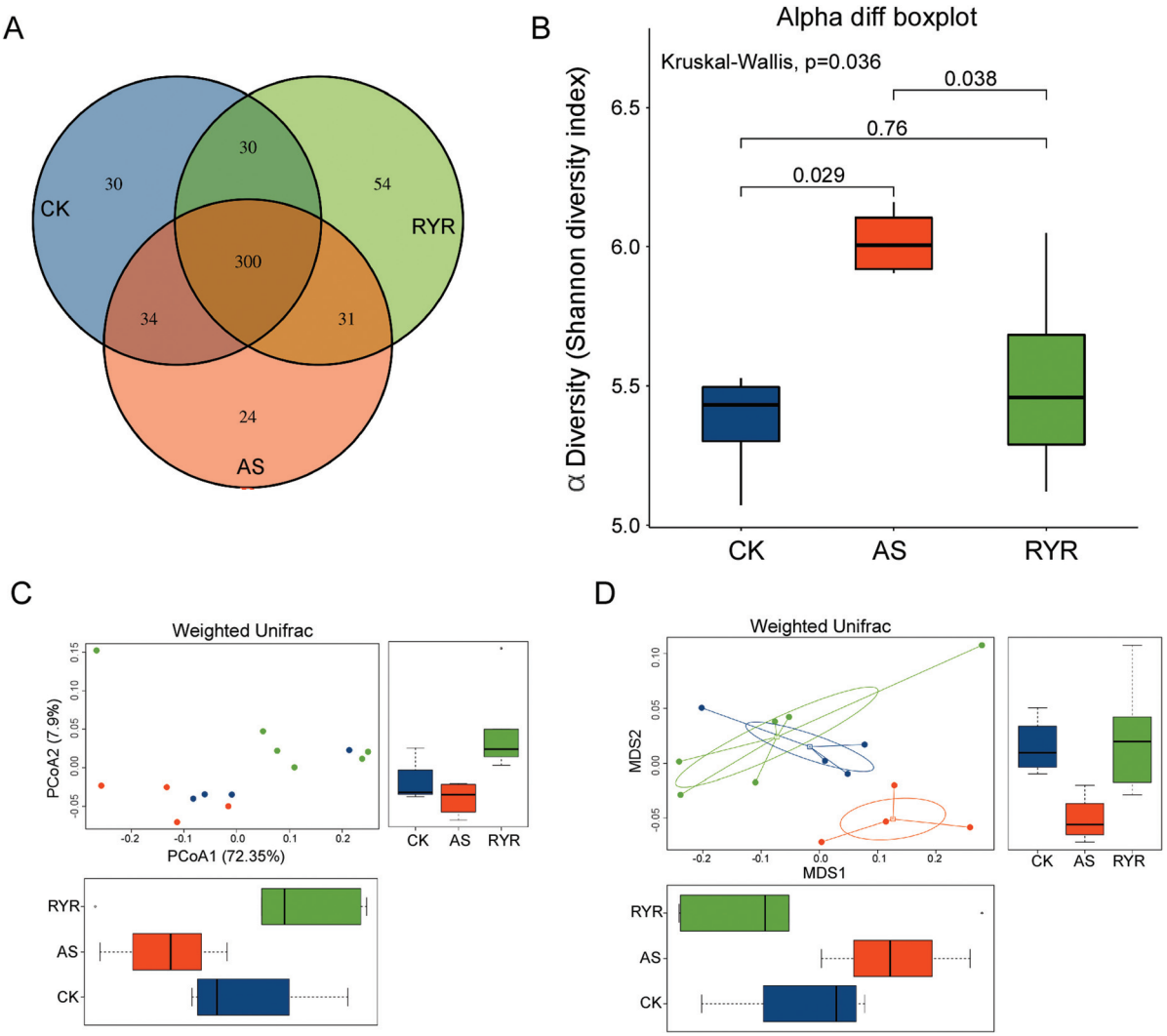

Fig. 3 Caecal gut microbiota diversity analysis. A, Venn diagram summarizing number of OTUs shared between different groups. B, Alpha diversity (Shannon index); beta diversity indicated by PCoA plot (C) and NMDS (D) of weighted UniFrac distance.

the protein levels of IL-1β, but negatively correlated with the protein levels of JAM-1. Moreover, the RYR induced increase in abundances of *Anaeroplasma* showed significant negative correlations with the plasma levels of LDL.

4. Discussion

Previous studies have identified that red yeast rice has an anti-inflammatory effect and reduces LDL and cholesterol in patients with dyslipidemia or atherosclerosis.[16,25,26] In the present study, we demonstrated that the high-fat diet-induced aorta plaque size and hypercholesterolemia could be significantly reduced by oral administration of RYR. Arterial observation by transmission electron microscopy confirmed the anti-atherosclerotic effects of RYR, which significantly reduced the harmful effect in intact endothelial cells induced by the high-fat diet. The lipid-lowering effects of RYR have been widely reported. For instance, Wu *et al.* reported that RYR could reduce the plaque size and decrease the serum levels of cholesterol.[27] It is known that *Monascus* produce a variety of functional secondary metabolites, among which monacolin compounds are marked to cause a reversible competitive inhibition of HMG-CoA reductase.[28] In addition, monacolin K, a major constitute of RYR, is structurally identical to lovastatin, which is the first statin drug to manage plasma lipids and prevent coronary heart disease.[29] HMG-CoA reductase is a rate-limiting enzyme in cholesterol biosynthesis. Further examination of the expression of HMG-CoA reductase also indicated that RYR displayed beneficial effects in suppressing the elevated HMG-CoA reductase levels in the livers of high-fat diet *Apoe*$^{-/-}$ mice, and thus reduced the plasma CHOL and LDL.

The intestinal epithelial barrier plays a critical role in restricting some gut bacteria-derived products (*e.g.*, LPS) into the systemic circulation, and high-fat diets usually lead to an increase in intestinal permeability.[30] Ghosh *et al.* have demon-

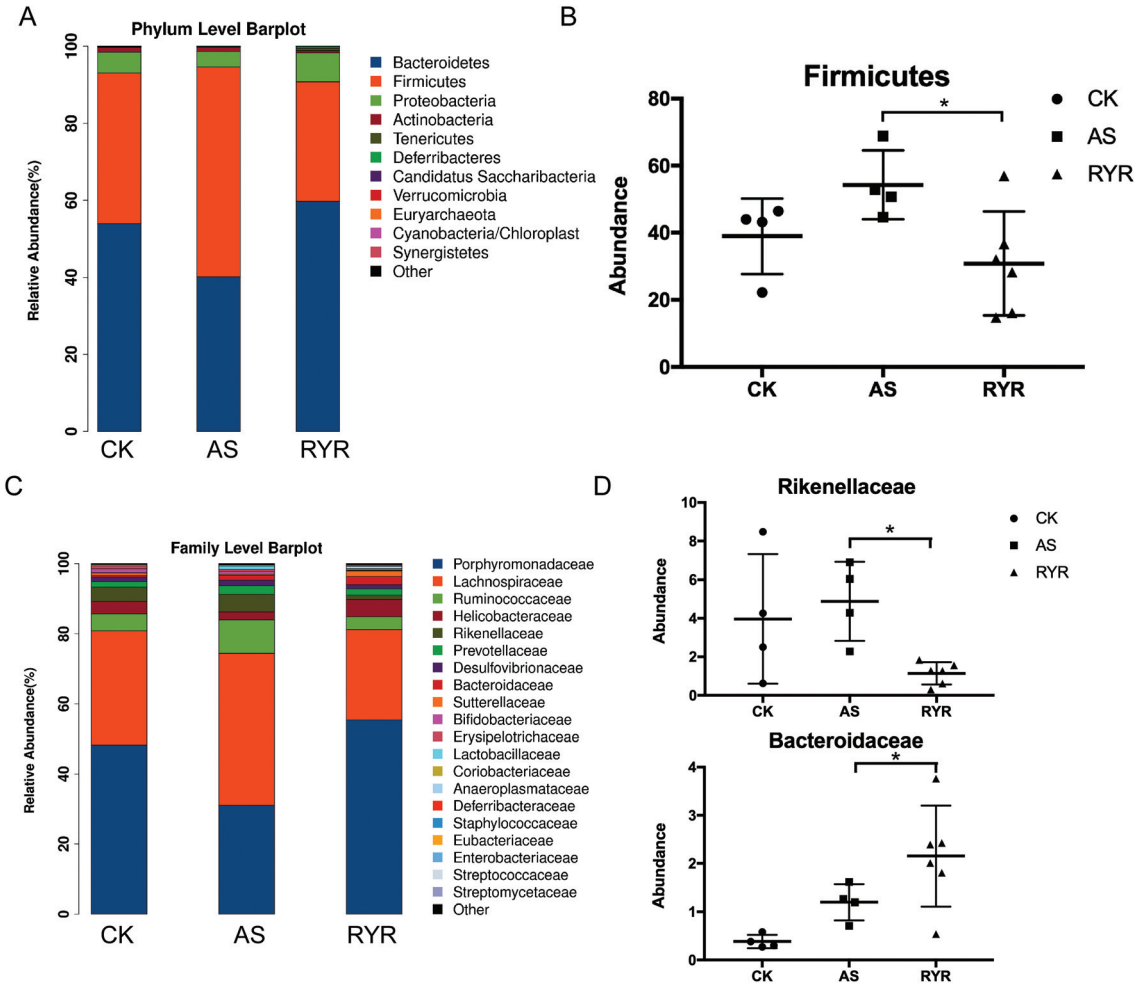

Fig. 4 Relative abundance of bacteria at the phylum and family level. One-way ANOVA with *LSD-t* test was applied to evaluate significant differences between the groups, $*p < 0.05$.

strated that oral supplementation with curcumin could prevent the development of metabolic diseases through regulating the intestinal barrier function.[31] In our study, we found that the RYR supplement could significantly improve the intercellular junction structure and the microvilli length compared with the high-fat diet group. Further western blot analysis of the tight junction proteins showed that the expression levels of JAM-1 and occludin proteins in the intestinal tissue of the *Monascus* group were significantly increased compared with the model group, revealing functions of RYR in improving high-fat diet-induced intestinal permeability.

Inflammation is another key etiological factor for atherosclerosis,[1] and anti-inflammatory interventions are widely applied to prevent atherosclerosis. For instance, Li *et al.* reported that *Akkermansia muciniphila* exhibited beneficial effects in the pathogenesis of atherosclerosis, evidenced by reduced inflammation.[32] We determined that the high-fat diet-induced inflammation in the intestinal tissues, as determined by western blot analysis of the expression of pro-inflammatory factors (TNF-α and IL-1β), was attenuated by treatment of $Apoe^{-/-}$ mice with RYR. This is consistent with recent research showing that supplementation with RYR in $Apoe^{-/-}$ mice decreased the plasma levels of IL-6 and TNF-α.[33] In order to elucidate the signal pathway responsible to RYR treatment, we examined the expression of proteins involved in inflammatory signaling pathways. Our results showed that TLR2, TLR4, and MAPK were significantly increased in the model group, whereas treatment with RYR reversed the increase of the three proteins. It is generally believed that activation of TLR4 not only stimulates the release of pro-inflammatory molecules from endothelial cells but also inhibits cholesterol efflux from macrophages and thus facilitates the foam cell formation.[32,34] Previous studies reported that deletion of TLR4 or TLR2 alone led to an obvious reduction of the aortic lesion area.[35,36] Here, we identified that RYR might combat atherosclerosis through modulating TLRs initiated MAPK signaling cascades, which is in agreement with previous reports that TLR4 and MAPK families were involved in the activation of circulating dendritic cells of acute coronary syndrome patients.[37]

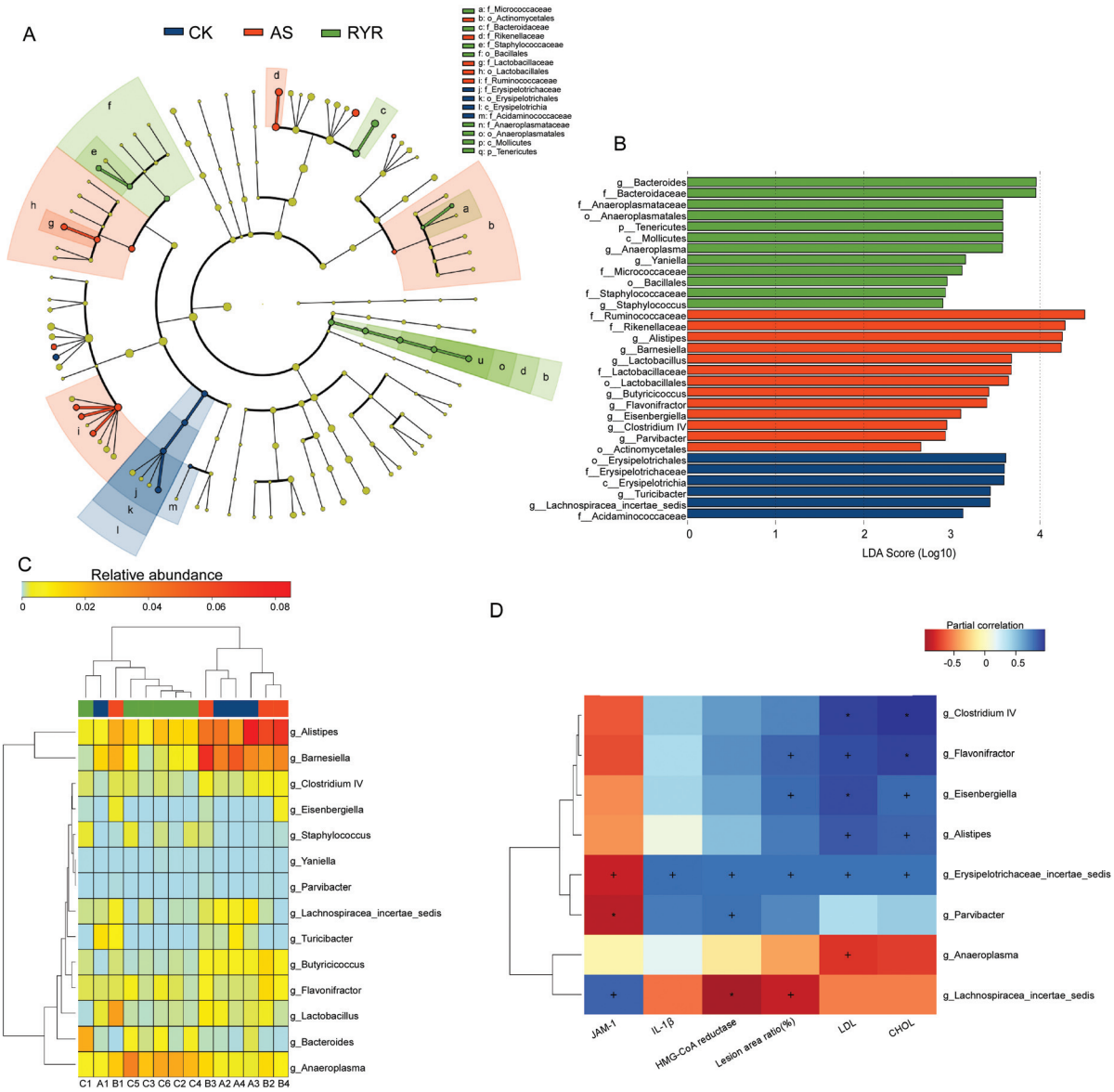

Fig. 5 The impact of RYR on the gut microbiota composition. A, Taxonomic cladogram generated by LEfSe analysis illustrating significant shifts in the gut microbiota in CK (blue), AS (red), or RYR (green) mice, respectively (n = 14). B, LDA scores of taxa (n = 14). C, Heat map comparison and hierarchical clustering dendrogram based on the relative abundance of 14 key genera across all treatment groups. D, Heat map describing the correlation of the abundances of key bacterial genera and atherosclerosis parameters. $+p < 0.05$, $*p < 0.01$.

In recent years, some studies have shown that alteration in gut microbiota are tightly linked to multiple pathological processes, including cardiovascular disease,[38,39] suggesting the gut microbiota as a potential therapeutic target for reducing metabolic disorder associated heart disease risks. So far, there are few reports on whether RYR administration influences the gut microbiota diversity in *Apoe*$^{-/-}$ mice or whether there are any associations between the altered gut microbiota profiling with atherosclerosis. Our current study demonstrated that RYR induced remarkable overall structural changes in the gut microbiota composition, which partially improves the dysbiosis of gut microbiota caused by the high-fat diet. The phylum *Firmicutes* was enriched due to the high-fat diet, whereas it was significantly decreased by the supplementation of RYR. It has been reported that the relative abundance of *Firmicutes* could contribute to the accumulation of metabolic endotoxins and inflammation,[40] which is consistent with our data. As mentioned before, *A. muciniphila* protected against atherosclerosis by preventing inflammation.[32] In addition, berberine treatment was found to lower intestinal expression of proinflammatory cytokines through increasing *Akkermansia* in the gut.[5] However, *Akkermansia* did not exhibit obvious alteration upon RYR treatment compared with the model group in our study, suggesting that the anti-inflammatory effect of RYR might not be contributed by *Akkermansia*. Notably, we found that RYR significantly increased the relative abundance of

Bacteroides, which is a group of short-chain fatty acid-producing bacteria that contribute to the beneficial effects against high-fat diet-induced obesity.[41,42] It is well known that *Bacteroides* confer numerous health benefits for the host;[43] for example, *B. fragilis* can deliver immunomodulatory molecules to human immune cells to protect from Crohn's disease.[44] However, when they escape from the gut they can cause significant pathology,[45] and *B. fragilis* secrete pro-inflammatory neurotoxins that are pathogenic to the central nervous system.[46] Therefore, it is essential to explore the molecular mechanisms underlying which some *Bacteroides* species is induced by RYR supplement to suppress atherosclerosis in the future. In addition, the abundance of *Alistipes* was markedly increased in the high-fat diet group, but partially decreased in the RYR group. Furthermore, *Alistipes* exhibited positive relationships with the plasma levels of CHOL and LDL according to Spearman's correlation analysis. Previous studies also revealed that increased *Alistipes* was associated with type-2 diabetes in humans and mice with heart failure.[47,48] Moreover, the increased abundance of gastrointestinal *Alistipes* was correlated with irritable bowel syndrome (IBS) and stress responses, such as depression.[49,50] Besides, our data showed that RYR treatment prompted the abundance of *Anaeroplasma*, which was negatively related to the plasma LDL. *Anaeroplasma* has been identified to be protective against atherosclerosis.[51] According to these findings, RYR might protect against high-fat diet-induced atherosclerosis through altering the gut microbiota diversity and composition.

In summary, our study adds to the accumulating evidence that red yeast rice attenuates high-fat diet-induced atherosclerosis, accompanied with decreased plaque size, plasma lipid levels, inflammation, and improvement of the gut barrier and gut microbiota structure. In addition, the MAPK pathway was elucidated to be involved in the anti-atherosclerotic effect of RYR. Our results further support the hypothesis that the underlying mechanisms of the anti-atherosclerotic effect of RYR are closely linked with the structural changes of gut microbiota. To our knowledge, this is the first study to show that RYR treatment specifically altered the abundance of *Alistipes* and *Anaeroplasma*, providing evidence for the possibility of pharmacological manipulation of the gut microbiota as a treatment for atherosclerosis. Nevertheless, there exist significant differences in physiology, metabolism and intestinal flora between mice and humans.[52] Further research is essential to explore the association between RYR and the abundance of *Alistipes* and *Anaeroplasma* in human gut flora, which will contribute to the development of functional foods and the clinical applications.

Author contributions

Liang H., Dong Y., and Cheng H. conceived and designed the experiments; Dong Y., Cheng H., and Xue M. performed the animal experiment and high throughput sequencing; Dong Y., Cheng H., and Liu Y. performed the experiments of western blot; Dong Y., Cheng H., and Liang H. analyzed the data; and Dong Y., Cheng H., and Liang H. drafted the manuscript. All authors read and approved this version for submission.

Conflicts of interest

The authors declare that the research was conducted in the absence of any commercial or financial relationships that could be construed as a potential conflict of interest.

Acknowledgements

This work was financially supported by National Natural Science Foundation of China (Grant No. 81573131, 31701733) and Shandong Provincial Natural Science Foundation, China (Grant No. ZR2016CQ31).

References

1 P. Libby, P. M. Ridker and A. Maseri, *Circulation*, 2002, **105**, 1135–1143.
2 H. Lu and A. Daugherty, *Curr. Opin. Lipidol.*, 2010, **21**, 552–553.
3 C. Matziouridou, N. Marungruang, T. D. Nguyen, M. Nyman and F. Fak, *Mol. Nutr. Food Res.*, 2016, **60**, 1150–1160.
4 G. K. Hansson, *N. Engl. J. Med.*, 2005, **352**, 1685–1695.
5 L. Zhu, D. Zhang, H. Zhu, J. Zhu, S. Weng, L. Dong, T. Liu, Y. Hu and X. Shen, *Atherosclerosis*, 2018, **268**, 117–126.
6 C. Erridge, *Trends Cardiovasc. Med.*, 2008, **18**, 52–56.
7 K. Takeda and S. Akira, *Semin. Immunol.*, 2004, **16**, 3–9.
8 J. C. Clemente, L. K. Ursell, L. W. Parfrey and R. Knight, *Cell*, 2012, **148**, 1258–1270.
9 J. M. Brown and S. L. Hazen, *Annu. Rev. Med.*, 2015, **66**, 343–359.
10 K. A. Krautkramer, J. H. Kreznar, K. A. Romano, E. I. Vivas, G. A. Barrett-Wilt, M. E. Rabaglia, M. P. Keller, A. D. Attie, F. E. Rey and J. M. Denu, *Mol. Cell*, 2016, **64**, 982–992.
11 D. Mozaffarian, E. J. Benjamin, A. S. Go, D. K. Arnett, M. J. Blaha, M. Cushman, S. R. Das, S. de Ferranti, J. P. Despres, H. J. Fullerton, V. J. Howard, M. D. Huffman, C. R. Isasi, M. C. Jimenez, S. E. Judd, B. M. Kissela, J. H. Lichtman, L. D. Lisabeth, S. Liu, R. H. Mackey, D. J. Magid, D. K. McGuire, E. R. Mohler 3rd, C. S. Moy, P. Muntner, M. E. Mussolino, K. Nasir, R. W. Neumar, G. Nichol, L. Palaniappan, D. K. Pandey, M. J. Reeves, C. J. Rodriguez, W. Rosamond, P. D. Sorlie, J. Stein, A. Towfighi, T. N. Turan, S. S. Virani, D. Woo, R. W. Yeh and M. B. Turner, *Circulation*, 2016, **133**, e38–360.
12 W. T. Fung, G. Subramaniam, J. Lee, H. M. Loh and P. H. Leung, *Sci. Rep.*, 2012, **2**, 298.
13 C. V. Venero, J. V. Venero, D. C. Wortham and P. D. Thompson, *Am. J. Cardiol.*, 2010, **105**, 664–666.
14 S. M. Ross, *Holist. Nurs. Pract.*, 2012, **26**, 173–175.

15 K. Wang, F. Liu, L. Y. Zhou, B. Long, S. M. Yuan, Y. Wang, C. Y. Liu, T. Sun, X. J. Zhang and P. F. Li, *Circ. Res.*, 2014, **114**, 1377–1388.
16 W. Zhou, R. Guo, W. Guo, J. Hong, L. Li, L. Ni, J. Sun, B. Liu, P. Rao and X. Lv, *Food Funct.*, 2019, **10**, 1073–1084.
17 A. P. Masella, A. K. Bartram, J. M. Truszkowski, D. G. Brown and J. D. Neufeld, *BMC Bioinf.*, 2012, **13**, 31.
18 R. C. Edgar, *Nat. Methods*, 2013, **10**, 996–998.
19 N. Segata, J. Izard, L. Waldron, D. Gevers, L. Miropolsky, W. S. Garrett and C. Huttenhower, *Genome Biol.*, 2011, **12**, R60.
20 D. W. Lachenmeier, Y. B. Monakhova, T. Kuballa, S. Lobell-Behrends, S. Maixner, M. Kohl-Himmelseher, A. Waldner and C. Steffen, *Chin. Med.*, 2012, **7**, 8.
21 G. Bazzoni and E. Dejana, *Physiol. Rev.*, 2004, **84**, 869–901.
22 T. Suzuki, *Cell. Mol. Life Sci.*, 2013, **70**, 631–659.
23 Y. K. Chan, M. S. Brar, P. V. Kirjavainen, Y. Chen, J. Peng, D. X. Li, F. C. C. Leung and H. El-Nezami, *BMC Microbiol.*, 2016, **16**, 264.
24 R. E. Ley, F. Backhed, P. Turnbaugh, C. A. Lozupone, R. D. Knight and J. I. Gordon, *Proc. Natl. Acad. Sci. U. S. A.*, 2005, **102**, 11070–11075.
25 S. P. Zhao, L. Liu, Y. C. Cheng and Y. L. Li, *Atherosclerosis*, 2003, **168**, 375–380.
26 C. W. Yang and S. A. Mousa, *Complement. Ther. Med.*, 2012, **20**, 466–474.
27 M. Wu, W. G. Zhang and L. T. Liu, *Chin. J. Integr. Med.*, 2017, **23**, 689–695.
28 G. Eisenbrand, *Mol. Nutr. Food Res.*, 2006, **50**, 322–327.
29 J. A. Tobert, *Nat. Rev. Drug Discovery*, 2003, **2**, 517–526.
30 P. D. Cani, R. Bibiloni, C. Knauf, A. Waget, A. M. Neyrinck, N. M. Delzenne and R. Burcelin, *Diabetes*, 2008, **57**, 1470–1481.
31 S. S. Ghosh, J. Bie, J. Wang and S. Ghosh, *PLoS One*, 2014, **9**, e108577.
32 J. Li, S. Lin, P. M. Vanhoutte, C. W. Woo and A. Xu, *Circulation*, 2016, **133**, 2434–2446.
33 M. Wu, W. G. Zhang and L. T. Liu, *Chin. J. Integr. Med.*, 2017, **23**, 689–695.
34 S. Kiechl, E. Lorenz, M. Reindl, C. J. Wiedermann, F. Oberhollenzer, E. Bonora, J. Willeit and D. A. Schwartz, *N. Engl. J. Med.*, 2002, **347**, 185–192.
35 X. Liu, T. Ukai, H. Yumoto, M. Davey, S. Goswami, F. C. Gibson 3rd and C. A. Genco, *Atherosclerosis*, 2008, **196**, 146–154.
36 K. S. Michelsen, M. H. Wong, P. K. Shah, W. Zhang, J. Yano, T. M. Doherty, S. Akira, T. B. Rajavashisth and M. Arditi, *Proc. Natl. Acad. Sci. U. S. A.*, 2004, **101**, 10679–10684.
37 L. Wang, D. Li, K. Yang, Y. Hu and Q. Zeng, *Immunology*, 2008, **125**, 122–130.
38 Z. Wang, E. Klipfell, B. J. Bennett, R. Koeth, B. S. Levison, B. Dugar, A. E. Feldstein, E. B. Britt, X. Fu, Y. M. Chung, Y. Wu, P. Schauer, J. D. Smith, H. Allayee, W. H. Tang, J. A. DiDonato, A. J. Lusis and S. L. Hazen, *Nature*, 2011, **472**, 57–63.
39 F. De Vadder, P. Kovatcheva-Datchary, D. Goncalves, J. Vinera, C. Zitoun, A. Duchampt, F. Backhed and G. Mithieux, *Cell*, 2014, **156**, 84–96.
40 D. I. Poppleton, M. Duchateau, V. Hourdel, M. Matondo, J. Flechsler, A. Klingl, C. Beloin and S. Gribaldo, *Front. Microbiol.*, 2017, **8**, 1215.
41 X. Zhang, Y. Zhao, M. Zhang, X. Pang, J. Xu, C. Kang, M. Li, C. Zhang, Z. Zhang, Y. Zhang, X. Li, G. Ning and L. Zhao, *PLoS One*, 2012, **7**, e42529.
42 X. Zhang, Y. Zhao, J. Xu, Z. Xue, M. Zhang, X. Pang and L. Zhao, *Sci. Rep.*, 2015, **5**, 14405.
43 A. G. Wexler and A. L. Goodman, *Nat. Microbiol.*, 2017, **2**, 17026.
44 H. Chu, A. Khosravi, I. P. Kusumawardhani, A. H. Kwon, A. C. Vasconcelos, L. D. Cunha, A. E. Mayer, Y. Shen, W. L. Wu, A. Kambal, S. R. Targan, R. J. Xavier, P. B. Ernst, D. R. Green, D. P. McGovern, H. W. Virgin and S. K. Mazmanian, *Science*, 2016, **352**, 1116–1120.
45 H. M. Wexler, *Clin. Microbiol. Rev.*, 2007, **20**, 593–621.
46 Y. Zhao, V. Jaber and W. J. Lukiw, *Front. Cell. Infect. Microbiol.*, 2017, **7**, 318.
47 H. Daniel, A. M. Gholami, D. Berry, C. Desmarchelier, H. Hahne, G. Loh, S. Mondot, P. Lepage, M. Rothballer, A. Walker, C. Bohm, M. Wenning, M. Wagner, M. Blaut, P. Schmitt-Kopplin, B. Kuster, D. Haller and T. Clavel, *ISME J.*, 2014, **8**, 295–308.
48 J. Qin, Y. Li, Z. Cai, S. Li, J. Zhu, F. Zhang, S. Liang, W. Zhang, Y. Guan, D. Shen, Y. Peng, D. Zhang, Z. Jie, W. Wu, Y. Qin, W. Xue, J. Li, L. Han, D. Lu, P. Wu, Y. Dai, X. Sun, Z. Li, A. Tang, S. Zhong, X. Li, W. Chen, R. Xu, M. Wang, Q. Feng, M. Gong, J. Yu, Y. Zhang, M. Zhang, T. Hansen, G. Sanchez, J. Raes, G. Falony, S. Okuda, M. Almeida, E. LeChatelier, P. Renault, N. Pons, J. M. Batto, Z. Zhang, H. Chen, R. Yang, W. Zheng, H. Yang, J. Wang, S. D. Ehrlich, R. Nielsen, O. Pedersen and K. Kristiansen, *Nature*, 2012, **490**, 55–60.
49 D. M. Saulnier, K. Riehle, T. A. Mistretta, M. A. Diaz, D. Mandal, S. Raza, E. M. Weidler, X. Qin, C. Coarfa, A. Milosavljevic, J. F. Petrosino, S. Highlander, R. Gibbs, S. V. Lynch, R. J. Shulman and J. Versalovic, *Gastroenterology*, 2011, **141**, 1782–1791.
50 A. Naseribafrouei, K. Hestad, E. Avershina, M. Sekelja, A. Linlokken, R. Wilson and K. Rudi, *Neurogastroenterol. Motil.*, 2014, **26**, 1155–1162.
51 Y. K. Chan, M. S. Brar, P. V. Kirjavainen, Y. Chen, J. Peng, D. Li, F. C. Leung and H. El-Nezami, *BMC Microbiol.*, 2016, **16**, 264.
52 M. Cheng, X. Zhang, Y. Miao, J. Cao, Z. Wu and P. Weng, *Food Res. Int.*, 2017, **92**, 9–16.